

# Electrogenerated Chemiluminescence. 72. Determination of Immobilized DNA and C-Reactive Protein on Au(111) Electrodes Using Tris(2,2'-bipyridyl)ruthenium(II) Labels

Wujian Miao and Allen J. Bard\*

Department of Chemistry and Biochemistry, 1 University Station A5300, The University of Texas at Austin, Austin, Texas 78712-0165

**Anodic electrogenerated chemiluminescence (ECL) with tri-*n*-propylamine (TPrA) as a coreactant was used to determine DNA and C-reactive protein (CRP) by immobilizations on Au(111) electrodes using tris(2,2'-bipyridyl)ruthenium(II) (Ru(bpy)<sub>3</sub><sup>2+</sup>) labels. A 23-mer synthetic single-stranded (ss) DNA derived from the *Bacillus anthracis* with an amino-modified group at the 5' end position was covalently attached to the Au(111) substrate precoated with a self-assembled thiol monolayer of 3-mercaptopropanoic acid (3-MPA) in the presence of 1-ethyl-3-(3-dimethylaminopropyl) carbodiimide hydrochloride (EDAC) and then hybridized with a target ssDNA tagged with Ru(bpy)<sub>3</sub><sup>2+</sup> ECL labels. Similarly, biotinylated anti-CRP species were immobilized effectively onto the Au(111) substrate precovered with a layer of avidin linked covalently via the reaction between avidin and a mixed thiol monolayer of 3-MPA and 16-mercaptohexadecanoic acid on Au(111) in the presence of EDAC and *N*-hydroxysuccinimide. CRP and anti-CRP tagged with Ru(bpy)<sub>3</sub><sup>2+</sup> labels were then conjugated to the surface layer. ECL responses were generated from the modified electrodes described above by immersing them in a TPrA-containing electrolyte solution. A series of electrode treatments, including blocking free –COOH groups with ethanol amine, pinhole blocking with bovine serum albumin, washing with EDTA/NaCl/Tris buffer, and spraying with inert gases, were used to reduce the nonspecific adsorption of the labeled species. The ECL peak intensity was linearly proportional to the analyte CRP concentration over the range 1–24 μg/mL. CRP concentrations of two unknown human plasma/serum specimens were measured by the standard addition method based on this technique.**

Studies on biosensors capable of rapidly, selectively, and sensitively detecting DNA sequences and antigen–antibody interactions have recently attracted much attention.<sup>1–11</sup> These kinds of biosensors, that is, DNA probe assays and immunoassays,

\* To whom correspondence should be addressed. Tel: (512) 471-3761. Fax: (512) 471-0088. Email: ajbard@mail.utexas.edu.

(1) Yang, V. C.; Ngo, T. T., Eds. *Biosensors and their Applications*, Kluwer Academic/Plenum Publishers: New York, 2000.

have a wide range of applications in areas of clinical diagnostics,<sup>3,10,11</sup> forensic chemistry,<sup>12,13</sup> environmental<sup>14,15</sup> investigations, pharmaceutical studies,<sup>12,16</sup> and biological warfare agent detections.<sup>17</sup> Many different types of techniques, such as electrochemical,<sup>1,2,4,5,14,18,19</sup> optical,<sup>1,2,8,11</sup> radiochemical,<sup>8</sup> piezoelectronic<sup>1,2,6,20</sup> and electrogenerated chemiluminescent (ECL) methods,<sup>10,21–25</sup> have been applied to accomplish these kinds of assays. ECL has many

- (2) Cunningham, A. J. *Introduction to Bioanalytical Sensors*, J. Wiley & Sons: New York, 1998.
- (3) Liron, Z.; Bromberg, A.; Fisher, M., Eds. *Novel Approaches in Biosensors and Rapid Diagnostic Assays*, Kluwer Academic/Plenum Publishers: New York, 2000.
- (4) Mikkelsen, S. R. *Electroanalysis* **1996**, *8*, 15–19.
- (5) Wang, J. *Anal. Chim. Acta* **2002**, *469*, 63–71.
- (6) Mannelli, I.; Minunni, M.; Tombelli, S.; Mascini, M. *Biosens. Bioelectron.* **2003**, *18*, 129–140.
- (7) Anderson, M. L. M. *Nucleic Acid Hybridization*, 1st ed.; Springer-Verlag: New York, 1998.
- (8) Sutherland, G.; Mulley, J. In *Nucleic Acid Probes*, Symons, R. H., Ed.; CRC Press: Boca Raton, FL, 1989; pp 159–201.
- (9) Park, S.-J.; Taton, T. A.; Mirkint, C. A. *Science* **2002**, *295*, 1503–1506.
- (10) Kenten, J. H.; Gudibande, S.; Link, J.; Willey, J. J.; Curfman, B.; Major, E. O.; Massey, R. J. *Clin. Chem.* **1992**, *38*, 873–879.
- (11) Christodoulides, N.; Tran, M.; Floriano, P. N.; Rodriguez, M.; Goodey, A.; Ali, M.; Neikirk, D.; McDevitt, J. T. *Anal. Chem.* **2002**, *74*, 3030–3036.
- (12) Heller, M. J. *Annu. Rev. Biomed. Eng.* **2002**, *4*, 129–153.
- (13) Nelson, M. S.; Benzinger, E. A.; Budzynski, M. J.; Boodee, M. T.; Matthews, A.; Buel, E.; Schwartz, M. B.; von Beroldingen, C.; Wampler, R. L.; et al. *J. Forensic Sci.* **1996**, *41*, 557–568.
- (14) Lucarelli, F.; Kicela, A.; Palchetti, I.; Marrazza, G.; Mascini, M. *Bioelectrochemistry* **2002**, *58*, 113–118.
- (15) Min, J.; Baeumner, A. J. *Anal. Biochem.* **2002**, *303*, 186–193.
- (16) Pollice, M.; Yang, H. L. *Clin. Lab. Med.* **1985**, *5*, 463–473.
- (17) Smith, W. D. *Anal. Chem.* **2002**, *74*, 462A–466A.
- (18) Campbell, C. N.; De Lumley-Woodyear, T.; Heller, A. F. *J. Anal. Chem.* **1999**, *364*, 165–169.
- (19) de Lumley-Woodyear, T.; Campbell, C. N.; Freeman, E.; Freeman, A.; Georgiou, G.; Heller, A. *Anal. Chem.* **1999**, *71*, 535–538.
- (20) Tombelli, S.; Mascini, M.; Turner, A. P. F. *Biosens. Bioelectron.* **2002**, *17*, 929–936.
- (21) Bard, A. J.; Debad, J. D.; Leland, J. K.; Sigal, G. B.; Wilbur, J. L.; Wohlsatdter, J. N. In *Encyclopedia of Analytical Chemistry: Applications, Theory and Instrumentation*; Meyers, R. A., Ed.; John Wiley & Sons: New York, 2000; Vol. 11, pp 9842–9849.
- (22) Fahrnich, K. A.; Pravda, M.; Guilbault, G. G. *Talanta* **2001**, *54*, 531–559.
- (23) Kenten, J. H.; Casadei, J.; Link, J.; Lupold, S.; Willey, J.; Powell, M.; Rees, A.; Massey, R. *Clin. Chem.* **1991**, *37*, 1626–1632.
- (24) Kijek, T. M.; Rossi, C. A.; Moss, D.; Parker, R. W.; Henchal, E. A. *J. Immunol. Methods* **2000**, *236*, 9–17.
- (25) Blackburn, G. F.; Shah, H. P.; Kenten, J. H.; Leland, J.; Kamin, R. A.; Link, J.; Peterman, J.; Powell, M. J.; Shah, A.; et al. *Clin. Chem.* **1991**, *37*, 1534–1539.

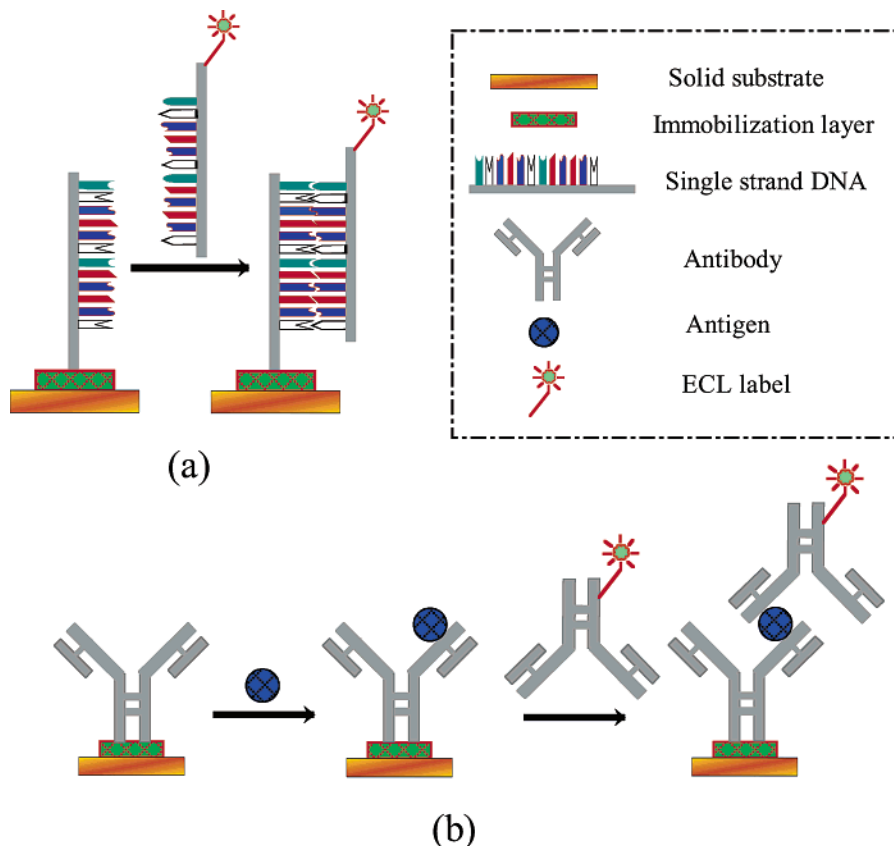


Figure 1. Schematic diagram of solid-state ECL detection of (a) DNA hybridization and (b) sandwich-type immunoassay.

distinct advantages over other detection systems.<sup>21,25</sup> For example, compared with fluorescence methods,<sup>8</sup> ECL does not involve a light source and, hence, the attendant problems of scattered light and luminescent impurities. Moreover, the specificity of the ECL reaction associated with the ECL label and the coreactant species decreases problems with side reactions and is characterized by good spatial and temporal resolution. Figure 1 illustrates the general principle of DNA probe assays and immunoassays based on ECL technique using ECL labels. Single stranded (ss) DNA or an antibody is first immobilized on the surface of the substrate (electrode), then the complementary ssDNA tagged with the ECL label (e.g., tris(2,2'-bipyridyl)ruthenium(II) or  $\text{Ru}(\text{bpy})_3^{2+}$ ) hybridizes with the confined ssDNA (Figure 1a), or the antigen combines with the immobilized antibody before it further couples with the antibody that is tagged with the ECL label (Figure 1b). When a potential is applied to the electrode in contact with a coreactant solution or scanned over a certain potential range, an ECL signal is generated and detected with a photomultiplier or CCD camera. The most widely used ECL label and coreactant are  $\text{Ru}(\text{bpy})_3^{2+}$  and tri-*n*-propylamine (TPrA), respectively, since the combination of these two gives the highest ECL efficiency in all coreactant ECL systems. As revealed in our recent study,<sup>26</sup> the ECL mechanism of the  $\text{Ru}(\text{bpy})_3^{2+}$ /TPrA system is complicated, and several routes associated with the generation of the excited-state  $\text{Ru}(\text{bpy})_3^{2+*}$  can be involved.

Most of the commercial ECL-based systems for bioassay reported so far, for example, the ORIGIN analyzer (IGEN, Inc.

Gaithersburg, MD), have used polystyrene-type magnetic beads ( $\sim 4 \mu\text{m}$  in diameter) as the immobilized support,<sup>10,21,23,25</sup> although more recent systems have involved immobilization on carbon supports.<sup>27</sup> For many applications, for example, chip<sup>28,29</sup> and disposable-type,<sup>30,31</sup> biosensors are more convenient. Au(111)<sup>32–35</sup> or Pt<sup>28</sup> coated silicon, glass, or mica wafers have been shown to be a good substrate for the immobilization of DNA and proteins, for example, via self-assembled thiol-COOH or thiol-NH<sub>2</sub> monolayers,<sup>33–40</sup> polymer films,<sup>18,19,40</sup> glyoxyl agarose,<sup>28,41,42</sup> and avidin/biotin interactions.<sup>43,44</sup> As will be discussed in the main text below,

(27) <http://meso-scale.com>.

(28) Sosnowski, R. G.; Tu, E.; Butler, W. F.; O'Connell, J. P.; Heller, M. J. *Proc. Natl. Acad. Sci. U.S.A.* **1997**, *94*, 1119–1123.

(29) Wang, J.; Pumera, M.; Chatrathi, M. P.; Rodriguez, A.; Spillman, S.; Martin, R. S.; Lunte, S. M. *Electroanalysis* **2002**, *14*, 1251–1255.

(30) Azek, F.; Grossiord, C.; Joannes, M.; Limoges, B.; Brossier, P. *Anal. Biochem.* **2000**, *284*, 107–113.

(31) Wang, J.; Tian, B.; Rogers, K. R. *Anal. Chem.* **1998**, *70*, 1682–1685.

(32) Xu, X.-H.; Bard, A. J. *J. Am. Chem. Soc.* **1995**, *117*, 2627–2631.

(33) Levicky, R.; Herne, T. M.; Tarlov, M. J.; Satija, S. K. *J. Am. Chem. Soc.* **1998**, *120*, 9787–9792.

(34) Patel, N.; Davies, M. C.; Hartshorne, M.; Heaton, R. J.; Roberts, C. J.; Tendler, S. J. B.; Williams, P. M. *Langmuir* **1997**, *13*, 6485–6490.

(35) Sun, X.; He, P.; Liu, S.; Ye, J.; Fang, Y. *Talanta* **1998**, *47*, 487–495.

(36) Aguilar, Z. P.; Vandaveer, W. R. I. V.; Fritsch, I. *Anal. Chem.* **2002**, *74*, 3321–3329.

(37) Caruso, F.; Rodda, E.; Furlong, D. N.; Niikura, K.; Okahata, Y. *Anal. Chem.* **1997**, *69*, 2043–2049.

(38) Huang, E.; Satjapipat, M.; Han, S.; Zhou, F. *Langmuir* **2001**, *17*, 1215–1224.

(39) Steel, A. B.; Levicky, R. L.; Herne, T. M.; Tarlov, M. J. *Biophys. J.* **2000**, *79*, 975–981.

(40) Herne, T. M.; Tarlov, M. J. *J. Am. Chem. Soc.* **1997**, *119*, 8916–8920.

(41) Cheng, J.; Sheldon, E. L.; Wu, L.; Uribe, A.; Gerrue, L. O.; Carrino, J.; Heller, M. J.; O'Connell, J. P. *Nat. Biotechnol.* **1998**, *16*, 541–546.

(26) Miao, W.; Choi, J.-P.; Bard, A. J. *J. Am. Chem. Soc.* **2002**, *124*, 14478–14485.

3-mercaptopropanoic acid (3-MPA) and the mixture of 3-MPA and 16-mercaptohexadecanoic acid were used in this report to form a thiol monolayer on Au for the immobilization of DNA and antibody (protein), respectively.

C-reactive protein (CRP) is a so-called "acute phase protein" found in human serum.<sup>45–48</sup> Concentrations of CRP are reported to be elevated up to 1000-fold (200  $\mu\text{g}/\text{mL}$ ) following injury, inflammation, or infection.<sup>48,49</sup> Numerous recent studies have demonstrated that CRP can be used to help predict the risk of acute events in patients with atherosclerosis.<sup>46,48,50–55</sup> CRP has also been shown to predict risk of future events in patients with acute coronary syndromes and in patients with stable angina and coronary artery stents.<sup>46–59</sup> As a result, CRP measurements could play a role as an assessor of risk factors for future coronary events.

In this paper, determinations of anthrax-related specific DNA sequences and CRP concentrations in human plasma/serum will be demonstrated using  $\text{Ru}(\text{bpy})_3^{2+}$  as the ECL labels and TPrA as the coreactant.

## EXPERIMENTAL SECTION

**Chemicals and Materials.** 3-Mercaptopropanoic acid (3-MPA) ( $\text{HS}(\text{CH}_2)_2\text{COOH}$ , 99+%), 16-mercaptohexadecanoic acid (16-MHA) ( $\text{HS}(\text{CH}_2)_{15}\text{COOH}$ , 90%), tris(2,2'-bipyridyl)ruthenium(II) dichloride hexahydrate ( $\text{Ru}(\text{bpy})_3\text{Cl}_2 \cdot 6\text{H}_2\text{O}$ ), ethanolamine (99+%), and tri-*n*-propylamine (TPrA, 99+%) from Aldrich (Milwaukee, WI); lithium perchlorate ( $\text{LiClO}_4$ , >99%) from Fluka (Milwaukee, WI); sodium phosphate dibasic heptahydrate ( $\text{Na}_2\text{HPO}_4 \cdot 7\text{H}_2\text{O}$ , 98.0%), sulfuric acid (98%), phosphoric acid ( $\text{H}_3\text{PO}_4$ , 85%), and methanol (spectroanalyzed grade) from Fisher (Fairlawn, NJ); potassium phosphate monobasic ( $\text{KH}_2\text{PO}_4$ , 99.6%) from J. T. Baker (Phillipsburg, NJ); tris(hydroxymethyl)aminomethane (Tris, ultrapure) from Life Technologies (Rockville, MD); 1-ethyl-3-(3-dimethylaminopropyl) carbodiimide hydrochloride (EDAC, SigmaUltra), *N*-hydroxysuccinimide (NHS), fluorescein biotin (90%), 1-methylimidazole, C-reactive protein (CRP, from human plasma), human plasma, anti-human C-reactive protein (anti-CRP, developed in rabbit,  $\sim 90$  mg/mL) from Sigma (St. Louis, MO); human serum from Cliniaq (Fallbrook, CA); sodium hydroxide, hydrochloric acid, and ethylenedinitrilotetraacetic acid (EDTA) from EM (Gibbstown, NJ); hydrogen peroxide (30%) from

Mallinckrodt (Hazelwood, MO); avidin (NeutrAvidin), bovine serum albumin (BSA), and sulfo-NHS-LC-biotin from Pierce (Rockford, IL);  $\text{Ru}(\text{bpy})_3^{2+}$  phosphoramidite<sup>10</sup> for DNA labeling and  $\text{Ru}(\text{bpy})_3^{2+}$ -NHS ester<sup>23,25</sup> for protein labeling from IGEN (Gaithersburg, MD); and ethanol (200-proof) from Aaper Alcohol (Shelbyville, KY) were used without further purification. Synthetic 23-mer single-stranded DNA (ss-DNA) oligonucleotides derived from the *Bacillus anthracis* (Ba813)<sup>60–62</sup> were obtained from Qiagen Operon (Alameda, CA) and had the following sequences: (a) probe or complementary, 5'- $\text{NH}_2$ -( $\text{CH}_2$ )<sub>6</sub>-AACGA TAGCT CCTAC ATTTG GAG-3' ( $\text{NH}_2$ -c-ss-DNA, MW = 7227 g/mol); (b) target, 5'-CTCCA AATGT AGGAG CTATC GTT-3' (t-ss-DNA, MW = 7039 g/mol); and (c) noncomplementary, 5'- $\text{NH}_2$ -( $\text{CH}_2$ )<sub>6</sub>-TTAAC ACCTT AGCGA CGGCT AGT-3' ( $\text{NH}_2$ -nc-ss-DNA, MW = 7203 g/mol). Gold-coated silicon wafers with a titanium adhesion layer were purchased from Platypus Technologies (Madison, WI). The thickness of the Au(111) thin layer was  $\sim 1000$  Å. The "inert dusting gas" with a main chemical component of 1,1,1,2-tetrafluoroethane was obtained from Techspray (Amarillo, TX). Compressed Ar, N<sub>2</sub>, and O<sub>2</sub> gases were supplied by Praxair (Danbury, CT). Unless otherwise stated, all solutions were freshly prepared with 18 M $\Omega$ -cm deionized Milli-Q water (Millipore Corp., Bedford, MA).

**Formation of Self-Assembled Monolayers (SAMs) on Au(111).** The gold-coated silicon wafers with dimensions of  $\sim 1$  to 2 cm<sup>2</sup> were cleaned using either a modified "UV/ozone-ethanol" method<sup>63</sup> or Piranha solution (98% H<sub>2</sub>SO<sub>4</sub>/30% H<sub>2</sub>O<sub>2</sub>, 70:30, v/v). In the former case, the wafers were placed in the chamber of a photochemical reactor (Southern New England Ultraviolet Co., Branford, CT) and irradiated with UV lamps for 20 min, followed by immersing the wafers in pure methanol for 30 min. In the later case, the wafers were immersed in a freshly prepared Piranha solution for 10–15 min, followed by washing with copious amounts of water before exposure to pure methanol (*CAUTION: Piranha solution can react violently with organic materials, and should be handled with extreme caution.*). Both cleaning methods provided satisfactory results. Comparing the two, the first method was used especially with lower quality gold films, since these films can sometimes peel off the Si substrates in Piranha solution if the adhesion layers are damaged due to the solution attack via "pinholes". The gold-coated Si wafers were subsequently washed thoroughly with water and ethanol and dried in a stream of argon before being transferred into a thiol solution.

Two types of self-assembled thiol monolayers were prepared in this investigation. For DNA studies, 3-MPA SAMs were formed on Au(111) by immersing the freshly cleansed gold-coated Si wafers for  $\sim 24$  h at room temperature in a 5 mM 3-MPA ethanol solution. For CRP determination, a mixed thiol-ethanol solution (5 mM 3-MPA and 5 mM 16-MHA, 10:1 v/v) was used to produce the mixed thiol SAMs. The newly formed Au(111)/SAM specimens were successively rinsed with ethanol and water and dried with argon before further use.

- (42) Guisan, J. M.; Bastida, A.; Blanco, R. M.; Garcia-Junceda, E. In *Immobilization of Enzymes and Cells*; Bickerstaff, G. F., Ed.; Humana Press: Totowa, New Jersey, 1997; pp 277–287.
- (43) Wilchek, M.; Bayer, E. A. *Anal. Biochem.* **1988**, *171*, 1–32.
- (44) Hermanson, G. T. *Bioconjugate Techniques*; Academic Press: New York, 1996.
- (45) Ablj, H. C.; Meinders, A. E. *Eur. J. Intern. Med.* **2002**, *13*, 412–422.
- (46) Du Clos, T. W. *Sci. Med.* **2002**, *8*, 108–117.
- (47) Volanakis, J. E. *Mol. Immunol.* **2001**, *38*, 189–197.
- (48) Benzaquen, L. R.; Yu, H.; Rifai, N. *Crit. Rev. Clin. Lab. Sci.* **2002**, *39*, 459–497.
- (49) Merritt, C. M.; Winkelman, J. W. *Anal. Chem.* **1989**, *61*, 2362–2365.
- (50) de Ferranti, S.; Rifai, N. *Clin. Chim. Acta* **2002**, *317*, 1–15.
- (51) Haidari, M.; Javadi, E.; Sadeghi, B.; Hajilooi, M.; Ghanbili, J. *Clin. Biochem.* **2001**, *34*, 309–315.
- (52) Heilbronn, L. K.; Clifton, P. M. *J. Nutr. Biochem.* **2002**, *13*, 316–321.
- (53) Ledue, T. B.; Rifai, N. *Clin. Chem. Lab. Med.* **2001**, *39*, 1171–1176.
- (54) Mortensen, R. F. *Immunol. Res.* **2001**, *24*, 163–176.
- (55) Rifai, N. *Card. Toxicol.* **2001**, *1*, 153–157.
- (56) Rifai, N.; Ridker, P. M. *Clin. Chem.* **2001**, *47*, 403–411.
- (57) Rifai, N.; Ridker, P. M. *Clin. Chem.* **2001**, *47*, 28–30.
- (58) Roberts, W. L.; Moulton, L.; Law, T. C.; Farrow, G.; Cooper-Anderson, M.; Savory, J.; Rifai, N. *Clin. Chem.* **2001**, *47*, 418–425.
- (59) Szalai, A. J. *Vasc. Pharm.* **2002**, *39*, 105–107.

- (60) Patra, G.; Sylvestre, P.; Ramiisse, V.; Therasse, J.; Guesdon, J.-L. *FEMS Immunol. Med. Microbiol.* **1996**, *15*, 223–231.
- (61) Patra, G.; Vaissaire, J.; Weber-Levy, M.; Le Doujet, C.; Mock, M. *J. Clin. Microbiol.* **1998**, *36*, 3412–3414.
- (62) Ramiisse, V.; Patra, G.; Vaissaire, J.; Mock, M. *J. Appl. Microbiol.* **1999**, *87*, 224–228.
- (63) Ron, H.; Matlis, S.; Rubinstein, I. *Langmuir* **1998**, *14*, 1116–1121.

**Modification of t-ssDNA and Anti-CRP with ECL Tag.** Ru(bpy)<sub>3</sub><sup>2+</sup>-labeled t-ssDNA was prepared by adding a 100-fold excess of Ru(bpy)<sub>3</sub><sup>2+</sup> phosphoramidite in 1 mL of MeCN to ~724 μg t-ssDNA in 0.5 mL of water. The mixture was shaken with a Vortex Genie 2 shaker (Fisher Scientific, Bohemia, NY), incubated at room temperature for ~1 h in the dark, and then transferred to a Sephadex G-25 PD-10 desalting column (Amersham Pharmacia Biotech, Piscataway, NJ) preequilibrated with 0.10 M PBS buffer solution (pH 7.4, 0.10 M sodium phosphate + 0.15 M NaCl) for product separation and purification according to the manufacturer's instructions. The eluted yellowish fraction was collected and diluted with 0.10 M PBS (pH 7.4) and stored at ~4 °C before use. The formation and concentration of Ru(bpy)<sub>3</sub><sup>2+</sup>-labeled DNA was identified by UV/vis absorption spectroscopy with a Spectronic 3000 array spectrophotometer (Milton Roy Co. Ivyland, PA) (see Results and Discussion Section for details). The DNA recovery rate after gel filtration was calculated to be ~88%. Neither hybridization kinetics nor hybrid stability of DNA should be affected by the labeling with the Ru(bpy)<sub>3</sub><sup>2+</sup> tag.<sup>10</sup> This approach was more convenient than DNA labeling with Ru(bpy)<sub>3</sub><sup>2+</sup> species carried out during the process of DNA synthesis,<sup>10,64</sup> which requires the use of an automated DNA synthesizer. Note that the use of a small amount of water during the course of the described DNA labeling was to increase the DNA solubility. However, the amount of water should be restricted, since water can react with Ru(bpy)<sub>3</sub><sup>2+</sup> phosphoramidite. For example, we found that the use of water can be avoided when labeling a 10-mer of DNA that was totally soluble in MeCN.

Similarly, the Ru(bpy)<sub>3</sub><sup>2+</sup>-labeled anti-CRP was obtained by adding 150 μg Ru(bpy)<sub>3</sub><sup>2+</sup> NHS ester predissolved in 30 μL DMSO to 1 mL of ~90 mg anti-CRP PBS solution (pH 7.2). After ~1 h incubation at room temperature in the dark, the mixture was filtered through a PD-10 column and eluted with 0.10 M PBS (pH 7.2). The purified Ru(bpy)<sub>3</sub><sup>2+</sup>-labeled anti-CRP was further diluted with PBS (pH 7.2) to 5.0 mL and kept at ~4 °C until use. This solution had an estimated anti-CRP concentration of ~15 mg/mL, with the assumption that the anti-CRP recovery rate was 83%.

#### **Biotinylation of Anti-CRP with Sulfo-NHS-LC-Biotin.**

Sulfo-NHS-LC-biotin is a water-soluble biotin with a spacer arm used to reduce steric hindrance of biotin and avidin binding interactions.<sup>44</sup> About 4.5 mg of sulfo-NHS-LC-biotin (MW = 556.6) was added to 1 mL of ~90 mg/mL anti-CRP PBS solution (pH 7.2), which corresponds to a 13:1 mole ratio of biotin to antibody, with the assumption that anti-CRP has a molecular weight of 150 kD/mol. The reaction was allowed to proceed for ~30 min at room temperature. Unbound biotin molecules were subsequently removed by a PD-10 column. The final product was stored in PBS (pH 7.2) solution at ~4 °C prior to use.

**Verification of Au(111)/SAM and Au(111)/SAM/Avidin Layer Formation.** It is necessary to ensure high quality of the thiol SAM- and SAM/avidin layers formed on the surface of Au(111) so that probe DNA and biotinylated anti-CRP can be effectively attached. About 10 μL of 25 μM avidin in 0.10 M 1-methylimidazole buffer (pH 7) containing 0.10 M EDAC and 0.10 M NHS was dropped onto a newly prepared Au(111)/3-MPA SAM or Au(111)/mixed thiol SAM. After incubation at 37 °C for

30 min, the modified wafer (electrode) was washed with water and dried with argon, and then the whole surface of the electrode was covered with 50 μL of 2.4 μM fluorescein biotin solution. The avidin-biotin reaction was again allowed to occur at 37 °C for 30 min, followed by successive washes with water and ethanol, and spray/dry with argon. Fluorescent images generated from the adsorbed fluorescein biotin were immediately taken with a Nikon Eclipse TE 300 inverted microscope (Nikon Instruments Inc., Melville, NY) coupled with a Magnafire model S99806 Olympus America CCD camera (Olympus America, Melville, NY) at λ<sub>ex</sub> ~ 490 nm and λ<sub>em</sub> ~ 520 nm.<sup>65</sup>

**Immobilization of Probe DNA and Anti-CRP onto the Au(111)/SAMs.** A schematic diagram showing the immobilization of the probe DNA (NH<sub>2</sub>-c-ssDNA) and anti-CRP onto the Au(111)/SAMs is given in Figure 2a and b, respectively. For DNA immobilization, 50 μL of 5 μM NH<sub>2</sub>-c-ssDNA in 0.10 M 1-methylimidazole buffer solution (pH 7) in the presence of freshly prepared 0.1 M EDAC was evenly distributed onto the surface of Au(111) covered with a 3-MPA thiol monolayer. The gold substrate was then incubated in an oven at a temperature of 37 °C for 30 min, followed by rinsing with copious amounts of water and ethanol and spraying/drying with argon. With this treatment, DNA was covalently bound to the Au(111) substrate, and physically adsorbed DNA was minimized. In the case of anti-CRP immobilization, a mixed thiol monolayer of 3-MPA and 16-MHA was chosen as a binding layer for avidin, since a previous study showed that a much higher surface coverage of protein can be achieved when mixed carboxylate-terminated SAMs were used in the presence of EDAC and NHS, as compared to a single thiol carboxylate-terminated SAM.<sup>34</sup> To obtain a layer of avidin, 50 μL of freshly prepared 25 μM NeutrAvidin in 0.10 M 1-methylimidazole buffer solution (pH 7) in the presence of 0.1 M EDAC and 0.1 M NHS was evenly distributed onto the surface of Au(111) covered with the mixed thiol monolayer of 3-MPA and 16-MHA, followed by incubation at 37 °C for 30 min, a thorough wash with water, and gas spray/dry with an argon stream. The Au(111)/mixed thiol SAM/avidin specimen obtained was subsequently covered with 50 μL of ~1.5 mg/mL biotinylated anti-CRP PBS solution (pH 7.2), and the avidin-biotin interactions were allowed to take place at 37 °C for 30 min. Unreacted antibodies were then removed from the substrate by washing with water and a spray/dry with argon. Note that Tris or phosphate buffers should not be used during the course of NH<sub>2</sub>-c-ssDNA or avidin reactions with carboxylate-terminated SAMs, since both Tris and phosphate can react with -COOH groups in the presence of EDAC,<sup>44</sup> resulting in insufficient immobilization of probe DNA and avidin on the surface of Au(111)/SAMs.

**DNA Hybridization and Sandwich-Type Biotinylated Anti-CRP < CRP > Ru(bpy)<sub>3</sub><sup>2+</sup> Labeled Anti-CRP Conjugate Formation.** Unless otherwise stated, all DNA hybridization and anti-CRP and CRP reactions were carried out at 37 °C for 30 min for each step. A 50-μL portion of each reagent was used. Solutions of target ssDNA and anti-CRP, both tagged with Ru(bpy)<sub>3</sub><sup>2+</sup>, were 5 μM in 0.10 M PBS (pH 7.4) and ~1.5 mg/mL in 0.10 M PBS (pH 7.2), respectively. Pure CRP samples were diluted with 0.10 M PBS (pH 7.2) prior to use, while human plasma samples

(64) Khan, S. I.; Beilstein, A. E.; Sykora, M.; Smith, G. D.; Hu, X.; Grinstaff, M. W. *Inorg. Chem.* **1999**, *38*, 3922–3925.

(65) Buranda, T.; Jones, G. M.; Nolan, J. P.; Keij, J.; Lopez, G. P.; Sklar, L. A. *J. Phys. Chem. B* **1999**, *103*, 3399–3410.

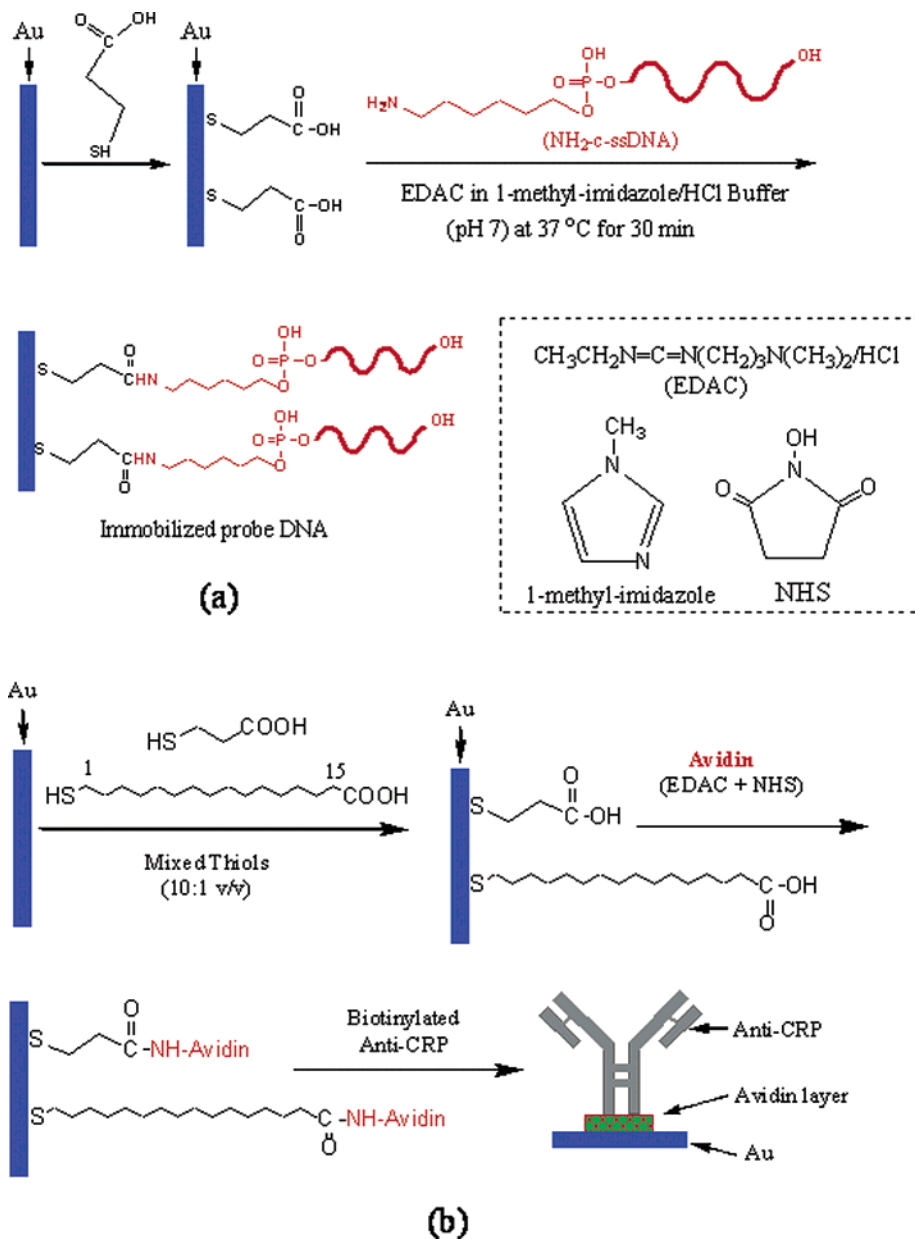


Figure 2. Schematic diagram showing (a) the immobilization of the probe DNA (NH<sub>2</sub>-c-ssDNA) onto the surface of Au(111)/3-MPA monolayer and (b) the attachment of anti-CRP onto the surface of Au(111)/mixed SAMs/avidin layer.

containing CRP were reconstituted with deionized water according to the manufacturer's instructions; human serum was used directly without any pretreatment. Procedures utilized to eliminate non-specific adsorption, for example, BSA blocking, ethanolamine reaction, and washing buffer incubation, were also carried out at 37 °C for 30 min for each process, unless stated otherwise.

The standard addition method was used to determine the CRP concentrations of the human plasma and serum samples. In each case, 0, 4.5 and 9.0  $\mu$ L of 100  $\mu$ g/mL standard CRP solutions were added to 150  $\mu$ L of the sample, respectively. A 50- $\mu$ L portion of the well-mixed CRP-containing solution was then used to form the above-described sandwich type conjugates, followed by ECL measurements.

**ECL and Electrochemical Measurements.** A homemade three-electrode cell, which had a configuration similar to that described previously,<sup>66</sup> was used with a Pt wire as the counter

electrode and a Ag/AgCl/KCl(sat.) electrode as the reference electrode. The Au(111) substrate immobilized with hybridized DNA/Ru(bpy)<sub>3</sub><sup>2+</sup> or sandwich type anti-CRP(CRP) anti-CRP-Ru(bpy)<sub>3</sub><sup>2+</sup> was used as the working electrode, which was exposed to the electrolyte solution (0.10 M LiClO<sub>4</sub>/0.10 M Tris/0.10 M TPrA, pH 8.0) via an O-ring and had an effective electrode area of  $\sim$ 0.28 cm<sup>2</sup>. The ECL along with the cyclic voltammogram (CV) signals were measured simultaneously with a home-built potentiostat combined with a photomultiplier tube (PMT, Hamamatsu R4220p, Japan) installed close to the electrochemical cell. A voltage of  $-750$  V was supplied to the PMT using a high-voltage power supply (Bertan High Voltage Corp., series 225, Hicksville, NY). All measurements were conducted at a temperature of  $20 \pm 2$  °C, unless otherwise stated.

(66) Xu, X.-H.; Bard, A. J. *Langmuir* **1994**, *10*, 2409–2414.

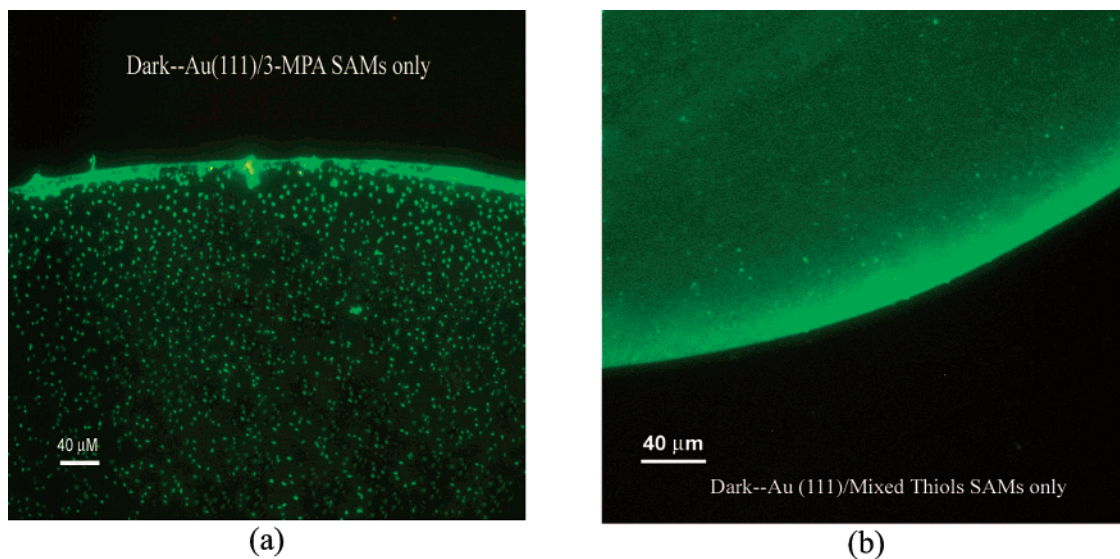


Figure 3. Fluorescent images obtained after the modification of (a) Au(111)/3-MPA/avidin and (b) Au(111)/mixed thiol SAM/avidin with fluorescein biotin species. The exposure times used were 3 and 30 s, respectively. The specimens were excited at  $\lambda_{\text{ex}} \sim 490$  nm and monitored at  $\lambda_{\text{em}} \sim 520$  nm.

## RESULTS AND DISCUSSION

**Fluorescent Images.** Figure 3a and b shows the fluorescent images obtained after the modification of fluorescein biotin onto the surface of Au(111)/3-MPA/avidin and Au(111)/mixed thiol SAM/avidin, respectively, as obtained with the inverted microscope. In both cases, green fluorescent images are clearly observed in the places where the avidin layers had been previously formed, in contrast to the dark parts where there were only SAMs. These results suggest that high quality of avidin layers were formed on the surface of Au(111)/SAMs [implying a good quality of the SAMs on the Au(111)]. Previous studies have revealed that a Au(111)/3-MPA SAM formed in aqueous perchloric acid solution was composed of molecularly ordered monolayer domains with a small number of defects<sup>67</sup> and that the extent of surface coverage of the protein, catalase, attached covalently to the Au(111)/SAMs by using EDAC/NHS strongly depended on the composition of the SAMs.<sup>34,68</sup> For example, among SAMs made with 3-MPA, 11-mercaptoundecanoic acid, and a mixture of the two thiols, the mixed SAMs gave the highest degree of protein immobilization, and 3-MPA the least. This behavior was attributed to the following two possible reasons:<sup>34</sup> First, the increased disorder of the mixed SAMs, resulting from either phase separation or full integration of the two thiol components, leads to terminal carboxylate groups that are more accessible for the immobilization of protein. Second, the increased hydrophobicity of the mixed SAM could promote hydrophobic interactions between the exposed methylene groups and the protein. The results shown in Figure 3 appear to be consistent with the results reported previously, although different exposure times were used for taking the two images. Note that along the edge of the Au(111)/SAM/avidin spot, a high intensity fluorescent strip was often observed (Figure 3a), suggesting that in this edge area, the surface concentration of avidin is higher than that in the bulk area. This is probably caused by a high

evaporation rate of water around the circle of a drop of avidin, resulting in the formation of a relatively high concentration of avidin in that region. A previous study<sup>69</sup> has indicated that covalently bound avidin may be covered by several layers of adsorbed avidin molecules and that the avidin was still biologically active when it was immobilized by cross-linker coupling.

**UV/Visible Absorption Spectra.** Figure 4 shows the UV/visible absorption spectra of a 23-mer target ssDNA (t-ssDNA, Figure 4a), Ru(bpy)<sub>3</sub><sup>2+</sup> labeled t-ssDNA (Figure 4c), and Ru(bpy)<sub>3</sub><sup>2+</sup> phosphoramidite tag itself (Figure 4b) in pH 7.4 PBS solutions. A characteristic absorption peak at  $\lambda_{\text{max}} \sim 260$  nm is observed for t-ssDNA (Figure 4a), and the concentration of this oligonucleotide ( $\sim 3.9 \mu\text{M}$ , MW = 7039 g/mol) can be quantified on the basis of the UV absorbance at 260 nm,  $A_{260 \text{ nm}} = 0.836$ , with a conversion factor of  $33 \mu\text{g mL}^{-1} \text{OD}^{-1}$ .<sup>70</sup> The absorption spectrum of the Ru(bpy)<sub>3</sub><sup>2+</sup> phosphoramidite exhibits the characteristic metal-to-ligand charge-transfer band (<sup>1</sup>MLCT) at  $\sim 457$  nm, similar to that in Ru(bpy)<sub>3</sub><sup>2+</sup> (Figure 4b). Other absorption peaks, including those at  $\lambda_{\text{max}} \sim 287$  nm and  $\lambda_{\text{max}} \sim 245$  nm, are also close to those obtained from Ru(bpy)<sub>3</sub><sup>2+</sup> and can be assigned to LC  $\pi \rightarrow \pi^*$  transitions and MLCT  $d \rightarrow \pi^*$  transitions, respectively.<sup>71</sup> Under the present experimental conditions, the molar extinction coefficient of Ru(bpy)<sub>3</sub><sup>2+</sup> phosphoramidite at  $\lambda_{\text{max}} = 457$  nm ( $\epsilon_{457}$ ) was calculated to be  $1.0 \times 10^4 \text{ M}^{-1} \text{cm}^{-1}$ , which is slightly smaller than that obtained from Ru(bpy)<sub>3</sub><sup>2+</sup> in aqueous solution ( $1.4 \times 10^4 \text{ M}^{-1} \text{cm}^{-1}$ ).<sup>71</sup> As shown in Figure 4c, after modification of t-ssDNA with Ru(bpy)<sub>3</sub><sup>2+</sup> phosphoramidite, a new absorption spectrum that includes both the DNA and Ru(bpy)<sub>3</sub><sup>2+</sup> characteristic absorption peaks is obtained, indicating that a Ru(bpy)<sub>3</sub><sup>2+</sup> segment has been attached to the DNA. The mole ratio of the DNA to the Ru (II) tag within the newly formed complex

(67) Sawaguchi, T.; Sato, Y.; Mizutani, F. *J. Electroanal. Chem.* **2001**, *507*, 256–262.

(68) Patel, N.; Davies, M. C.; Heaton, R. J.; Roberts, C. J.; Tendler, S. J. B.; Williams, P. M. *Appl. Phys. A* **1998**, *A66*, S569–S574.

(69) Achtnich, U. R.; Tiefenauer, L. X.; Andres, R. Y. *Biosens. Bioelectron.* **1992**, *7*, 279–290.

(70) QIAGEN—Operon. *Product Guide 2002*; QIAGEN Inc.: Alameda, CA, 2002. www.qiagen.com.

(71) Juris, A.; Balzani, V.; Barigelletti, F.; Campagna, S.; Belser, P.; Von Zelewsky, A. *Coord. Chem. Rev.* **1988**, *84*, 85–277.

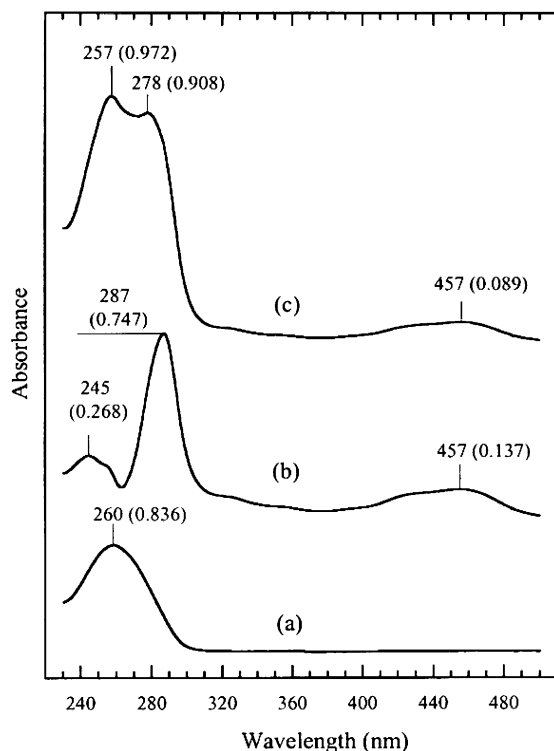


Figure 4. UV/vis absorption spectra obtained for (a) 23-mer t-ssDNA (see main text), (b) 13.3  $\mu\text{M}$   $\text{Ru}(\text{bpy})_3^{2+}$  phosphoramidite, and (c) t-ssDNA tagged with  $\text{Ru}(\text{bpy})_3^{2+}$  species in 0.10 M PBS (pH 7.4) using a 1-cm cuvette.

was calculated as 1:2 on the basis of the absorbance values at  $\lambda_{\text{max}} \sim 257$  nm for DNA and  $\lambda_{\text{max}} \sim 457$  nm for Ru (II). This molar ratio is consistent with the fact that both the 5'- and 3'-terminals of the t-ssDNA contain hydroxyl groups after automated synthesis.<sup>70</sup> That is, both DNA terminals have been covalently bound with one  $\text{Ru}(\text{bpy})_3^{2+}$  species.

**Strategies Used to Reduce Nonspecific Adsorption.** One of the great challenges in DNA and immunoassays is the elimination of nonspecific adsorption of the labeled species. A number of factors, such as "pinholes" of the self-assembled monolayer and electrostatic interactions with unreacted terminal groups of the SAM, could cause this kind of adsorption.  $\text{Ru}(\text{bpy})_3^{2+}$  itself can strongly adsorb onto Au, Pt, and HOPG electrodes and thereby produce ECL signals in the presence of TPrA.<sup>66</sup> This sort of adsorption can be significantly reduced (by  $\sim 50\%$ ) by spraying the electrode with an inert gas, as shown by the ECL vs potential profiles (see Supporting Information for details). In addition to the "inert dusting gas", which has a main chemical component of 1,1,1,2-tetrafluoroethane and nitrogen, argon, oxygen, and compressed air all showed a similar effect, suggesting that nonspecifically adsorbed  $\text{Ru}(\text{bpy})_3^{2+}$  species were probably physically flushed by the gas used. Similar trends were also observed for  $\text{Ru}(\text{bpy})_3^{2+}$ -labeled t-ssDNA species nonspecifically adsorbed on Au(111) with and without coverage of 3-MPA monolayer (not shown). This removal of adsorbed species by a strong gas flow is quite surprising, and the mode and limits of this behavior are being investigated further.

The nonspecific adsorption of  $\text{Ru}(\text{bpy})_3^{2+}$ -labeled t-ssDNA species on Au(111)/3-MPA monolayer can be further reduced significantly by pretreatment of the electrode with either a 0.10

M ethanolamine/EDAC (0.10 M 1-methylimidazole, pH 7) or a 2% BSA (0.10 M PBS, pH 7.4) solution (Table 1), demonstrating that compared to  $-\text{COOH}$  groups, newly formed terminal  $-\text{OH}$  groups and a possible thin layer of BSA over the 3-MPA monolayer discourage adsorption of  $\text{Ru}(\text{bpy})_3^{2+}$ -labeled species. "Pinholes" on Au(111)/SAMs could entrap  $\text{Ru}(\text{bpy})_3^{2+}$  labeled species and cause significant nonspecific adsorption, which may be eliminated by utilizing BSA blocking agent. By combining both ethanolamine/EDAC and BSA blocking agent, smaller nonspecific ECL signals were observed, as expected (Table 1). Schematic diagrams showing the blocking principle behind the Au(111)/SAM electrode pretreatment with ethanolamine and BSA, along with the possible existence of "pinhole" and free  $-\text{COOH}$  groups after the covalent immobilization of amino-modified ssDNA onto the Au(111)/SAM electrode are given in the Supporting Information section.

Additionally, after DNA hybridization and sandwich-type antibody-antigen conjugate formation, nonspecific adsorption of the  $\text{Ru}(\text{bpy})_3^{2+}$ -labeled species can also be dramatically reduced by incubation of the electrode in a washing buffer solution (5 mM Tris/HCl-0.5 mM EDTA-1.0 M NaCl, pH 7.5) at 37  $^\circ\text{C}$  for 15 to 30 min (not shown). The flowcharts in Figure 5 outline all of the protocol involved in the electrode treatment for the determination of immobilized DNA (Figure 5a) and CRP (Figure 5b) using  $\text{Ru}(\text{bpy})_3^{2+}$  as ECL labels.

**ECL Detection of DNA Hybridization.** Figure 6 shows the ECL intensity vs potential profiles along with the CV obtained for the detection of immobilized DNA on Au(111) using  $\text{Ru}(\text{bpy})_3^{2+}$  labels. Clearly, the complementary DNA hybrid (Figure 6a), in which the probe ssDNA is  $\text{NH}_2$ -c-ssDNA, and the target ssDNA is t-ssDNA tagged with  $\text{Ru}(\text{bpy})_3^{2+}$  (see the Experimental Section for details), gives a much higher ECL response with respect to that for the noncomplementary DNA (Figure 6b), in which the probe ssDNA ( $\text{NH}_2$ -nc-ssDNA) had as many as 4 complementary base-pair matches with the t-ssDNA. As in the case presented in Figure 6, the ECL intensity obtained from the noncomplementary DNA hybridization, that is, the nonspecific adsorption, was generally  $\sim 10\%$  relative to that obtained from the complementary DNA hybridization. Instead of 2% BSA, a number of surfactants with various concentrations, such as 0.25% cetyltrimethylammonium bromide and sodium dodecyl sulfate, and 0.5% Triton X-100 and Tween-20, were also tested for reduction of nonspecific adsorption. The results revealed that these surfactants can, indeed, reduce the nonspecific adsorption, as suggested previously,<sup>35,72</sup> but they can also greatly inhibit the complementary DNA hybridization, resulting in even higher percentages of signal from nonspecific adsorption, as compared to the test sample. In a separate experiment, we observed  $\sim 20$  to 30% signal from nonspecific adsorption when probe DNA was electrostatically immobilized onto Au(111)/3-MPA SAM attached with Al (III) species. No significant improvement was found when using the avidin-biotin configuration to immobilize the probe DNA to the surface of either the Au(111)/3-MPA SAM or the Au(111)/mixed thiol SAM, although a previous study indicated this kind of immobilization could provide higher sensitivity for the detection of the hybridization reaction, with negligible nonspecific adsorption.<sup>20</sup>

(72) Liu, S.; Ye, J.; He, P.; Fang, Y. *Anal. Chim. Acta* **1996**, *335*, 239-243.

Table 1. Protocol Used for the Reduction of Nonspecific Adsorption of Ru(bpy)<sub>3</sub><sup>2+</sup>-Labeled ssDNA<sup>a</sup> (ssDNA–Ru(II)) on Au(111)/3-MPA<sup>b</sup> Monolayer (Au/SAM)

| no. | treatment <sup>c</sup>                                    | possible functions                                    | I <sub>ECLp</sub> (nA) <sup>d</sup> (± 10%) |
|-----|---|---|---|
| A   | Au/SAM + ssDNA-Ru(II)                                     |   | over 240                                    |
| B   | Au/SAM + 0.10 M ethanolamine/EDAC + ssDNA-Ru(II)          | blocking –COOH groups                                 | 34  |
| C   | Au/SAM + 2% BSA + ssDNA-Ru(II)                            | blocking “pinholes” and formation of a thin BSA layer | 21  |
| D   | Au/SAM + 0.10 M ethanolamine/EDAC + 2% BSA + ssDNA-Ru(II) | B + C   | 16  |

<sup>a</sup> ssDNA was a 23-mer single-stranded DNA with the following sequence: 5'-CTCCA AATGT AGGAG CTATC GTT-3', and the molar ratio of the ssDNA to Ru(bpy)<sub>3</sub><sup>2+</sup> in labeled ssDNA was 1:2 (see main text for details). <sup>b</sup> 3-MPA stands for 3-mercaptopropionic acid. <sup>c</sup> Washing with water + ethanol + gas spray (Ar) three times between each step, incubation at 37 °C for 60 min for each reaction step. <sup>d</sup> ECL was carried out in 0.10 M TPrA/0.10 M LiClO<sub>4</sub>/0.10 M Tris (pH 8) solutions between 0 and 1.10 V vs Ag/AgCl at a scan rate of 50 mV/s. The ECL peak potentials were around + 0.90 to + 0.95 V vs Ag/AgCl.

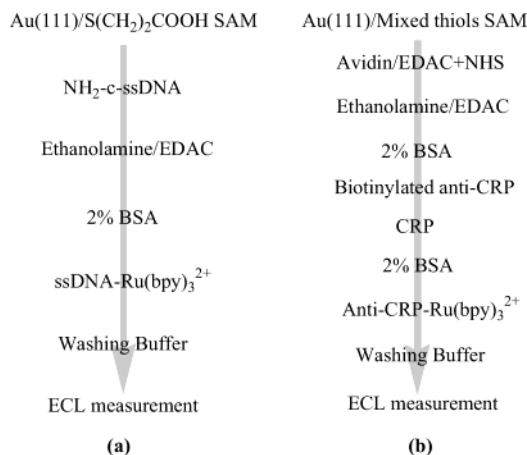


Figure 5. Flowcharts showing all of the processes involved in the electrode treatment for the determination of immobilized DNA (a) and CRP (b) using Ru(bpy)<sub>3</sub><sup>2+</sup> as ECL labels.

As shown in Figure 6, only one ECL peak, located at ~0.95 V vs Ag/AgCl, is observed for both complementary and noncomplementary DNA hybridizations. This peak potential is close to the anodic peak potential for TPrA oxidation at a bare Au or glassy carbon electrode (~0.85 to 0.95 V vs Ag/AgCl) but significantly less positive than that of the free Ru(bpy)<sub>3</sub><sup>2+</sup> oxidation (~1.1 V vs Ag/AgCl) under similar experimental conditions,<sup>26,73</sup> suggesting that the observed ECL responses in Figure 6 are most likely generated from Ru(bpy)<sub>3</sub><sup>2+</sup> that is formed by the redox reaction between TPrA<sup>•+</sup> (the cation radical) produced during TPrA oxidation and Ru(bpy)<sub>3</sub><sup>+</sup> produced from the reduction of Ru(bpy)<sub>3</sub><sup>2+</sup> by TPrA<sup>•+</sup> (the free radical formed by proton loss).<sup>26</sup> This finding is consistent with our previous studies,<sup>26,73</sup> in which the predominant ECL signals originated from TPrA, rather than Ru(bpy)<sub>3</sub><sup>2+</sup>, oxidation when low concentrations of Ru(bpy)<sub>3</sub><sup>2+</sup> (~≤ μM) were used, as in the case of our current study. Note also that the cyclic electrochemical responses at Au(111)/3-MPA SAM electrode immobilized with DNAs are essentially the same and are generally a reflection of TPrA oxidation, since its concentration (0.10 M in the bulk) is significantly higher than any other electroactive species at the electrode surface.

**Determination of C-Reactive Protein.** The ECL and CV responses of the Au(111)/mixed thiols SAM/avidin electrode with conjugated anti-CRP tagged with Ru(bpy)<sub>3</sub><sup>2+</sup> in the presence of

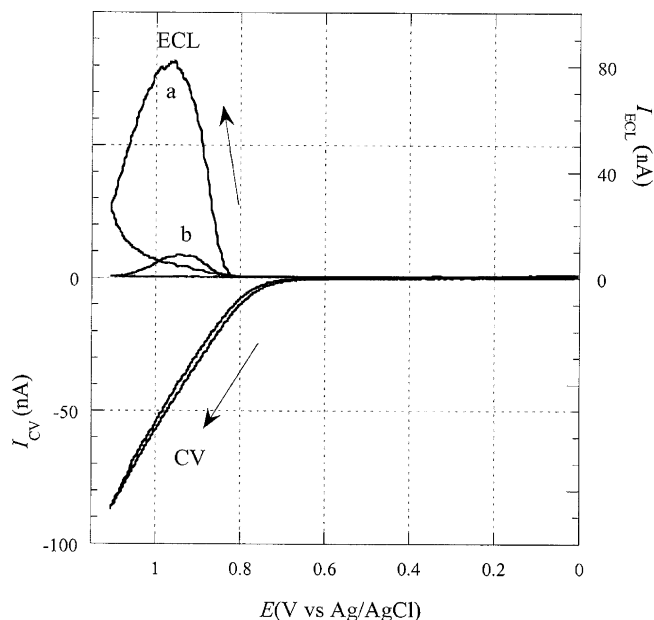


Figure 6. ECL intensity vs potential profiles along with the cyclic voltammogram (CV) obtained for the detection of immobilized DNA on Au(111) using Ru(bpy)<sub>3</sub><sup>2+</sup> labels. (a) Complementary DNA hybridization. (b) Noncomplementary DNA hybridization. The CVs for both (a) and (b) were essentially the same; only one is displayed here. ECL experiments were carried out in 0.10 M TPrA/0.10 M LiClO<sub>4</sub>/0.10 M Tris (pH 8) electrolyte solutions at a scan rate of 50 mV/s. Each ssDNA used had a 23-mer sequence.

TPrA are shown in Figure 7. As expected, these responses are very similar to those obtained from the DNA hybridizations (Figure 6), since in both cases, the ECL label and the electrolyte used are essentially the same. Very low levels of nonspecific adsorption of labeled anti-CRP were always observed (~5 nA). In the specific case of Figure 7, nonspecific adsorption (Figure 7b) was ~1.5% of the signal from the test sample (Figure 7a). A good correlation between the CRP concentration and the ECL peak intensity with a wide dynamic range (1–24 μg/mL CRP) that covers most of the CRP levels in human plasmas and serums (0.2–15 μg/mL<sup>56–58,74</sup>, with a mean value<sup>75</sup> of 1.9 μg/mL for men and 2.0 μg/mL for women) was also observed (Figure 8). Thus, on the basis of this standard curve, the ECL approach should be

(74) Roberts, W. L.; Sedrick, R.; Moulton, L.; Spencer, A.; Rifai, N. *Clin. Chem.* **2000**, *46*, 461–468.

(75) Onat, A.; Sansoy, V.; Yildirim, B.; Keles, I.; Uysal, O.; Hergenc, G. *Am. J. Cardiol.* **2001**, *88*, 601–607.

(73) Zu, Y.; Bard, A. J. *Anal. Chem.* **2000**, *72*, 3223–3232.



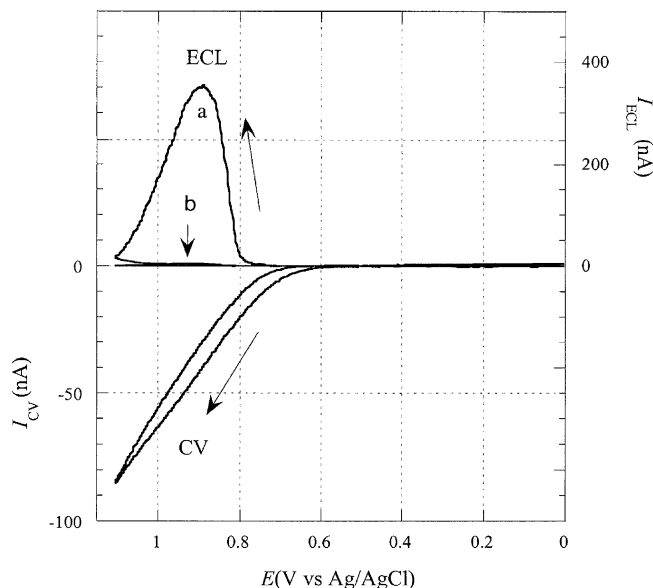


Figure 7. ECL intensity vs potential profiles along with the cyclic voltammogram (CV) obtained for the determination of immobilized C-reactive protein (CRP) on Au(111) using Ru(bpy)<sub>3</sub><sup>2+</sup> labels: (a) with a CRP concentration of 23.5 μg/mL and (b) background (nonspecific adsorption) of anti-CRP–Ru(bpy)<sub>3</sub><sup>2+</sup>. The CVs for both (a) and (b) were essentially the same; only one is displayed here. ECL experiments were carried out in 0.10 M TPrA/0.10 M LiClO<sub>4</sub>/0.10 M Tris (pH 8) electrolyte solutions at a scan rate of 50 mV/s.

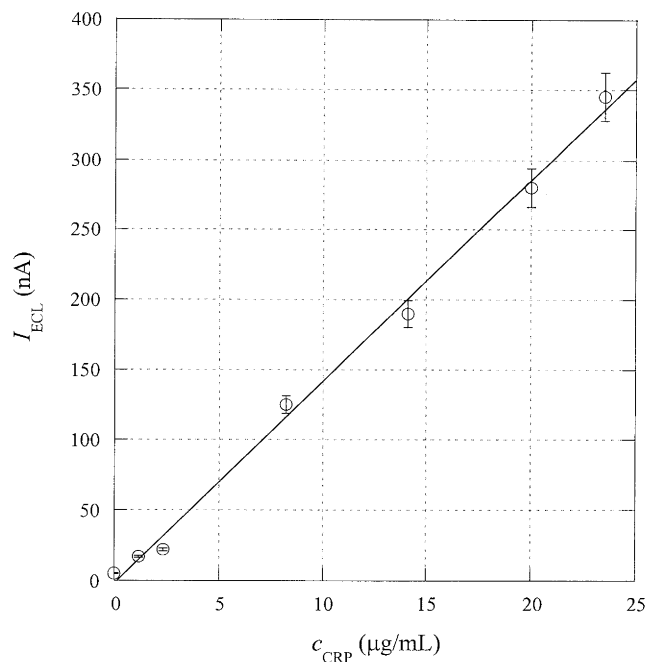


Figure 8. Correlation between the CRP concentration and the ECL peak intensity. ECL experiments were conducted in 0.10 M TPrA/0.10 M LiClO<sub>4</sub>/0.10 M Tris (pH 8) electrolyte solutions between 0 and 1.10 V vs Ag/AgCl at a scan rate of 50 mV/s.

useful for the determination of CRP concentrations in plasma and serum samples. To increase the determination accuracy and, more importantly, to examine the validity of this protocol, a standard addition method was applied to measure the CRP concentrations of two unknown human plasma/serum samples. As shown in Figure 9, a good linear relationship between a human serum sample obtained from Cliniqa Corp. (Figure 9a) or a human

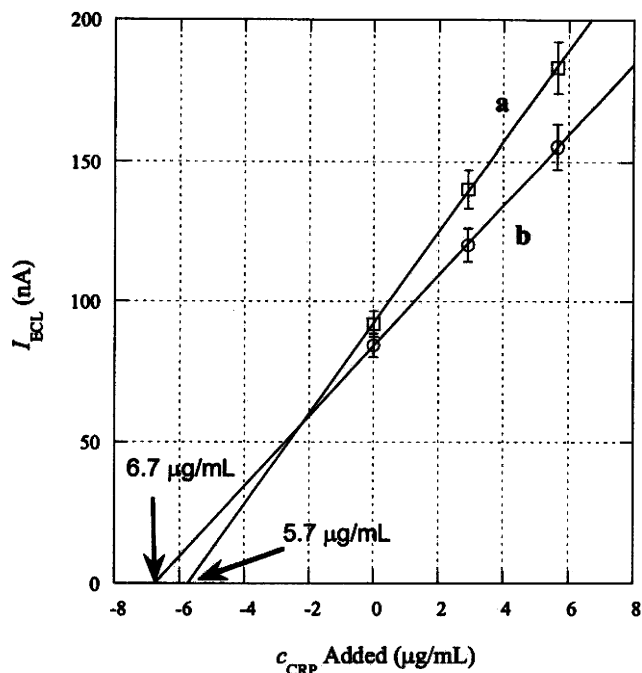


Figure 9. Determination of the CRP concentration in (a) human serum obtained from Cliniqa Corp. and (b) human plasma obtained from Sigma using standard addition method. On the basis of the assumption that the nonspecific adsorption of the Ru(bpy)<sub>3</sub><sup>2+</sup>-tagged anti-CRP is the same in serum, plasma, and PBS buffer, a 5 nA ECL current was used to correct the nonspecific adsorption effect. The experimental conditions were as in Figure 8.

plasma sample obtained from Sigma (Figure 9b) with added standard CRP concentrations and the ECL peak intensities is evident. The calculated CRP concentrations for these two unknown samples, 5.7 μg/mL and 6.7 μg/mL, respectively, are very close to those values obtained directly from the standard curve shown in Figure 8. According to the criteria suggested by Rifai et al.,<sup>56,57</sup> these two blood donors may be placed in the class of the highest cardiovascular risk. The different slopes obtained for lines a and b in Figure 9 are probably due to a matrix effect, since compared with serum, human plasma samples generally contain extra components, such as protein fibrinogen, which may weaken the affinity between the anti-CRP and CRP. As a result, ECL data obtained for the plasma sample show a relatively smaller slope (Figure 9b) compared to that for the serum one (Figure 9a).

## CONCLUSIONS

Amino-modified ssDNA can be covalently attached to the Au(111) substrate precovered with a thiol monolayer of 3-MPA in the presence of EDAC and then hybridized with a target ssDNA tagged with Ru(bpy)<sub>3</sub><sup>2+</sup> ECL labels. Similarly, biotinylated anti-CRP can be effectively immobilized onto the Au(111) substrate precovered with a layer of avidin produced covalently via the reaction between avidin and a mixed thiol monolayer of 3-MPA and 16-MHA on Au(111) in the presence of EDAC and NHS. CRP and anti-CRP tagged with Ru(bpy)<sub>3</sub><sup>2+</sup> ECL labels can be subsequently attached by conjugation. The DNA hybridization and the formation of sandwich-type anti-CRP(CRP)anti-CRP–Ru(bpy)<sub>3</sub><sup>2+</sup> conjugates can be verified by anodic ECL responses using TPrA as a coreactant. The ECL peak intensity was linearly proportional to the analyte CRP concentration in a range of 1–24 μg/mL. This

standard curve can be directly used for the determination of unknown CRP samples. Alternatively, CRP concentrations of unknown specimens, for example, human plasma/serum, can be measured by the standard addition method based on the ECL technique. Nonspecific adsorption of the labeled species can be significantly reduced by using a series of electrode treatments, such as blocking free  $-\text{COOH}$  groups with ethanolamine, pinhole blocking with BSA, washing with EDTA/NaCl/Tris buffer, and spraying with inert gases. In principle, the technique demonstrated in this paper should be applicable to the determination of other immobilized DNA hybridizations and formation of antibody-antigen conjugates on the electrode surfaces.

#### ACKNOWLEDGMENT

This work has been supported by grants from IGEN and MURI-DAAD 19-99-1-0207.

#### SUPPORTING INFORMATION AVAILABLE

Effect of gas spray on reduction of nonspecific  $\text{Ru}(\text{bpy})_3^{2+}$  adsorption on Au(111). Schematic diagrams showing the blocking principle behind the Au(111)/SAM electrode pretreatment with ethanolamine and BSA, along with the possible existence of "pinhole" and free  $-\text{COOH}$  groups after the covalent immobilization of amino-modified ssDNA onto the Au(111)/SAM electrode. This material is available free of charge via the Internet at <http://pubs.acs.org>.

Received for review June 2, 2003. Accepted August 8, 2003.

AC034596V